AN INVESTIGATION INTO THE INTERFERENCE REJECTION CAPABILITY OF A LINEAR ARRAY IN A WIRELESS COMMUNICATIONS SYSTEM

Salman Durrani and Marek E. Bialkowski
School of Information Technology and Electrical Engineering
University of Queensland
Brisbane, QLD. 4072, Australia

Received 15 June 2002

ABSTRACT: *The suitable use of an array antenna at the base station of a wireless communications system can result in improvement in the signal-to-interference ratio (SIR). In general, the SIR is a function of the direction of arrival of the desired signal and depends on the configuration of the array, the number of elements, and their spacing. In this paper, we consider a uniform linear array antenna and study the effect of varying the number of its elements and inter-element spacing on the SIR performance.* © 2002 Wiley Periodicals, Inc. Microwave Opt Technol Lett 35: 445–449, 2002; Published online in Wiley InterScience (www.interscience.wiley.com). DOI 10.1002/mop.10634

Key words: *smart antennas; linear array antennas; wireless communications; interference rejection*

1. INTRODUCTION

In recent years, a lot of interest has been shown in smart antennas with respect to existing and future wireless communications systems. An attractive feature of the smart array antenna is that when suitable weights are applied to the signals received by individual antenna elements, the discrimination of the receiver against undesired/interfering signals, in comparison with a single antenna system, can considerably be improved. Before developing a smart antenna system it is important to assess the potential of a given array configuration to reject the interference. An important performance measure in this regard is the interference rejection or SIR improvement capability. This capability of rejection of undesired signals is in general a function of the array geometry (for example, linear or circular), the number of antenna elements (including their spacing), and the direction of signal arrival of the desired user and the interferers. It is defined as a reciprocal of the spatial interference suppression coefficient, which is determined as an average cross-correlation between the array-steering vector toward a given user and the steering vector toward the interferers. In many papers, addressing the topic of smart antennas, the SIR improvement capability of an antenna array has been only vaguely addressed [1, 2, 3].

In this paper we provide a detailed presentation of the SIR improvement ability of a uniform linear array, which, for example, can be located on one side of a triangular panel as part of a larger base-station antenna system. In particular, we consider the effect of varying the number of antenna elements and the inter-element spacing on the SIR improvement. Due to the applied signal processing method, these considerations are valid for an array operating within the code division multiple access (CDMA) system. However, the findings can be extended for alternative access systems.

2. THEORY

Consider a linear array of N antenna elements, which forms one side of a triangular panel array of the base station and is located at the origin of the Cartesian coordinate system. The array receives M narrowband signals from mobile users, which are randomly distributed in the azimuthal direction (the xy or $\theta = 90°$ plane). For simplicity, we consider a uniform linear array (ULA) of omnidirectional antenna elements, spaced a distance $d = \lambda/2$ along the x-axis. We assume that with regard to this array the users are located in the far-field region. In this case, the parameter that characterizes the location of the source is its direction of arrival (DOA) ϕ, or alternatively ψ, which is conventionally measured from the array broadside, as shown in Figure 1. The received signal at the mth antenna can be expressed as

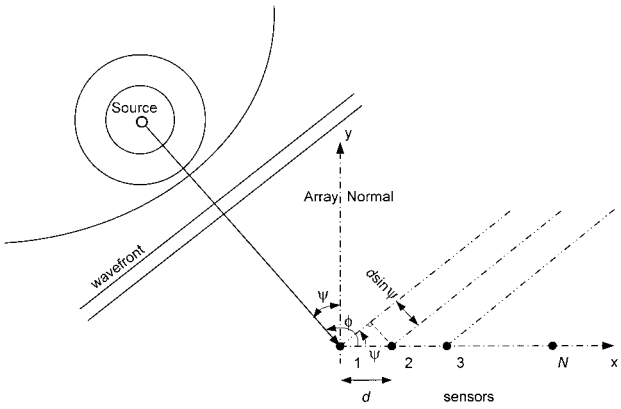

Figure 1 Array geometry for an N element uniform linear array with inter-element spacing d

$$x_m(t) = \sum_{k=1}^{M} s_k(t) e^{-j2\pi(d_m/\lambda_c)\sin\psi_k} + n_m(t), \tag{1}$$

where d_m = distance between the mth and reference antenna element (element number 1), $s_k(t)$ = signal transmitted by the kth source as received by the reference antenna, ψ_k = angle of arrival of the kth source as measured from the array broadside, λ_c = carrier frequency wavelength of the signals, and $n_m(t)$ = additive white Gaussian noise at the antenna arrays with zero mean and variance σ^2. Using vector notation, Eq. (1) can be expressed as

$$\mathbf{x}(t) = \sum_{k=1}^{M} \mathbf{a}(\psi_k) s_k(t) + \mathbf{n}(t) = \mathbf{A}(\psi_k)\mathbf{s}(t) + \mathbf{n}(t), \tag{2}$$

where $\mathbf{x}(t) = [x_1(t), x_2(t), \ldots, x_N(t)]^T$ is $N \times 1$ vector of measured voltages, $\mathbf{s}(t) = [s_1(t), s_2(t), \ldots, s_M(t)]^T$ is $M \times 1$ signal vector, $\mathbf{n}(t) = [n_1(t), n_2(t), \ldots, n_N(t)]^T$ is $N \times 1$ noise vector, $\mathbf{A}(\psi) = [\mathbf{a}(\psi_1), \mathbf{a}(\psi_2), \ldots, \mathbf{a}(\psi_M)]$ is $N \times M$ steering matrix whose columns are steering vectors of the sources and $(\cdot)^T$ denotes transpose operation.

The array correlation matrix $\mathbf{R}_{xx}$, associated with vector $\mathbf{x}(t)$, contains information about how signals from each element are correlated with each other and is given by

$$\mathbf{R}_{xx}(t) = E[\mathbf{x}(t)\mathbf{x}^H(t)], \tag{3}$$

where $E[\cdot]$ denotes expectation or statistical averaging operator.

The $N \times 1$ steering vector $\mathbf{a}(\psi_k)$ models the spatial response of the array due to an incident plane wave from the ψ_k direction. In general, it is the product of antenna response $H(\psi)$ and the geometrical array factor [4] and is given as

$$\mathbf{a}(\psi_k) = [H_1(\psi_k)\ H_2(\psi_k)e^{-jkd\sin\psi_k}\ H_3(\psi_k)e^{-j2kd\sin\psi_k} \cdots\ H_N(\psi_k)e^{-j(N-1)kd\sin\psi_k}]^T, \quad (4)$$

where $H_n(\psi_k)$ denotes the response of antenna element n and $(\cdot)^T$ denotes transpose operation.

If mutual coupling between antenna elements is neglected and the individual element patterns are identical, then scaling them with respect to element number 1 reduces Eq. (4) to

$$\mathbf{a}(\psi_k) = [1\ e^{-jkd\sin\psi_k}\ e^{-j2kd\sin\psi_k} \cdots\ e^{-j(N-1)kd\sin\psi_k}]^T. \quad (5)$$

Note that when the mutual coupling is neglected the steering vector, as given by Eq. (4), is independent of the actual types of elements forming the array. This justifies our assumption that omnidirectional antenna elements constitute the considered linear array.

The collection of these steering vectors over the parameter set of interest $\Re = \{\mathbf{a}(\psi)|\psi \in \Theta\}$ is called the array manifold, where Θ denotes the set of all possible parameter vectors. The array manifold is assumed to be unambiguous, that is, the matrix $\mathbf{A}(\psi)$ has full rank for all distinct $\psi_k \in \Theta$. It can be shown that the uniform linear array manifold is unambiguous if the direction of arrivals (DOAs) are confined to the set $\Theta = [-\pi/2, \pi/2]$ as in [5].

Let $s_1(t)$ be the desired signal source arriving from the direction ψ_1 and consider the rest of the signals $s_k(t)$, $k = 2, \ldots, M$ as interferences arriving from the respective directions. The array output is given by

$$y(t) = \mathbf{w}^H\mathbf{x}(t), \quad (6)$$

where $\mathbf{w}$ is the weight vector that is applied to the antenna array to produce a beam pattern with its main lobe in the direction of the desired user and $(\cdot)^H$ denotes Hermitian (complex conjugate) transpose.

For a conventional beamformer, all the weights are of equal magnitudes while phases are selected to steer the array in a particular direction known as look direction. In a CDMA signal environment, where the desired signal is dominant due to the CDMA signal processing gain, we can use the eigenvector e_1, corresponding to the maximum eigenvalue λ_1 of the array correlation matrix $\mathbf{R}_{xx}$, as the value of the weight vector to track the desired user [1]. Thus, $\mathbf{w}$ is given by

$$\mathbf{w} = \frac{1}{\sqrt{N}}\mathbf{a}(\psi_1) \quad (7)$$

and the array becomes the phased array as the magnitudes of the weight vector are constant and only phases are varying.

Substituting this value in Eq. (6), and using Eq. (1) and simplifying, we get

$$y(t) = s_1(t) + \frac{1}{N}\sum_{k=2}^{M} s_k(t)\mathbf{a}^H(\psi_1)\mathbf{a}(\psi_k) + \frac{1}{N}\mathbf{a}^H(\psi_1)\mathbf{n}(t). \quad (8)$$

The mean output power of the processor is

$$P(t) = E[\,y(t)\,y*(t)]$$

$$= E[|s_1(t)|^2] + \sum_{k=2}^{M}\frac{1}{N^2}|\mathbf{a}^H(\psi_1)\mathbf{a}(\psi_k)|^2E[|s_k(t)|^2] + E\left[\frac{1}{N}|\mathbf{a}^H(\psi_1)\mathbf{n}(t)|^2\right]$$

$$= E[|s_1(t)|^2] + \sum_{k=2}^{M}\alpha_k(\psi_1,\ \psi_k)\,E[|s_k(t)|^2] + \frac{\sigma_n^2}{N}, \quad (9)$$

where $\alpha_k(\psi_1,\ \psi_k) = (1/N^2)|\mathbf{a}^H(\psi_1)\mathbf{a}(\psi_k)|^2$.

The first term on the right side of Eq. (9) is the desired signal power, whereas the second and third terms represent interference and noise power, respectively.

The Signal-to-Noise ratio (SNR) at the array output ($\mathrm{SNR_o}$) can be written as

$$\mathrm{SNR_o} = \frac{E[|s_1(t)|^2]}{E\left[\frac{1}{N}|\mathbf{a}^H(\psi_1)n(t)|^2\right]} = N\frac{E[|s_1(t)|^2]}{\sigma^2} = N(\mathrm{SNR_{in}}), \quad (10)$$

where σ^2 denotes noise power, while $\mathrm{SNR_{in}}$ is the signal to noise ratio at the input of each antenna element. Eq. (10) shows that the SNR at the array output is improved N times or by 10 log 10(N) in dB.

The SIR at the array output ($\mathrm{SIR_o}$) can be written as

$$\mathrm{SIR_o} = \frac{E[|s_1(t)|^2]}{\sum_{k=2}^{M}\alpha_k(\psi_1,\ \psi_k)\,E[|s_k(t)|^2]}. \quad (11)$$

We see that the SIR at the array output is a function of ψ_1, the direction of the desired user. The mean SIR at the array output ($\mathrm{SIR_o}$) can be written in terms of input SIR ($\mathrm{SIR_{in}}$) [2] as

$$\mathrm{SIR_o} = \frac{\mathrm{SIR_{in}}}{G_{avg}(\psi_1)}, \quad (12)$$

where $G_{avg}(\psi_1)$ is the spatial interference suppression coefficient. Assuming ψ_k is uniformly distributed in the range $[-\pi/2, \pi/2]$ (meaning that the interfering signals are equally probable from any direction in the specified range), it is given as the mean value of $\alpha_k(\psi_1, \psi_k)$ by

$$G_{avg}(\psi_1) = E[\alpha_k(\psi_1, \psi_k)] = \frac{1}{\pi}\int_{-\pi/2}^{\pi/2}\alpha_k(\psi_1, \psi_k)d\psi_k, \quad (13)$$

where

$$\alpha_k(\psi_1, \psi_k) = \left|\frac{\mathbf{w}^H}{\|\mathbf{w}^H\|}\frac{\mathbf{a}(\psi_k)}{\|\mathbf{a}(\psi_k)\|}\right|^2 = \frac{1}{N^2}|\mathbf{a}^H(\psi_1)\mathbf{a}(\psi_k)|^2 \quad (14)$$

and $\|\cdot\|$ is the vector norm. Substituting the values from Eq. (5), and using the equality $\sum_{x=0}^{X-1} a^x = (1 - a^X)/(1 - a)$ and simplifying, we get

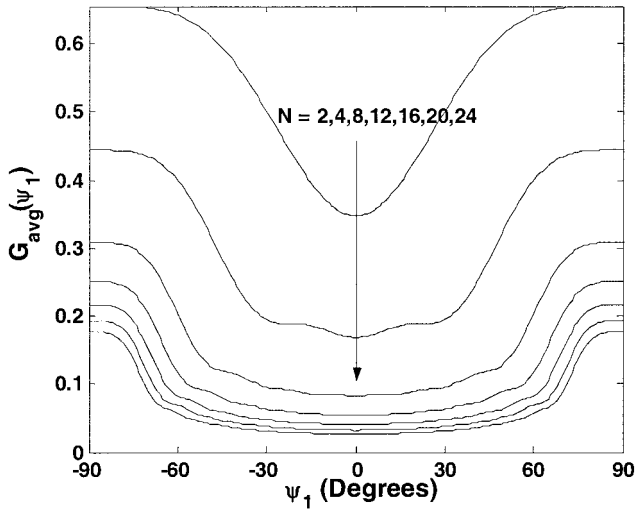

Figure 2 Plot of variation of spatial interference suppression coefficient $G_{avg}(\psi_1)$ with direction of arrival (DOA) of desired user ψ_1 for different number of antenna elements N with $d = 0.5\lambda$

$$\alpha_k(\psi_1, \psi_k) = \frac{1}{N^2} \frac{\left|\sin\left(\frac{\pi N}{2}(\sin\psi_1 - \sin(\psi_k)\right)\right|^2}{\left|\sin\left(\frac{\pi}{2}(\sin\psi_1 - \sin(\psi_k)\right)\right|^2}. \quad (15)$$

From Eq. (15), we see that coefficient $\alpha_k(\psi_1, \psi_k)$ depends on the difference between the sines of the angles rather than on the difference between the angles themselves. Therefore, $G_{avg}(\psi_1)$ and SIR_o depend on the value of the steered angle ψ_k.

The average improvement in SIR (Δ) at the array output is then given as

$$\Delta = 10 \log 10\left(\frac{1}{G_{avg}(\psi_1)}\right) = -10 \log 10(G_{avg}(\psi_1)). \quad (16)$$

3. RESULTS AND DISCUSSION

First we investigate the effect of varying the number of antenna elements N on the spatial interference suppression coefficient $G_{avg}(\psi_1)$. The inter-element spacing is set to $d = \lambda/2$. Figure 2 shows the plot of $G_{avg}(\psi_1)$ for a linear array for different N. The curves are U-shaped, with a broad minimum, implying that interference reduction is maximum over a certain range of ψ_1, centred at $\psi_1 = 0°$ (broadside). However, the exact amount of SIR at the array output is dependent on ψ_1. The presented result conforms to the expectation that a linear array's discrimination against interferers (in terms of SIR) is best in its broadside direction and deteriorates in its end-fire direction, for example, given an $N = 12$ element array, the average improvement in SIR at the array output is $\Delta = 12.65$ dB for $\psi_1 = 0°$ (broadside) and only 6 dB for $\psi_1 = 90°$ (end-fire).

To characterise this degradation in performance, we can define an "interference reduction beamwidth" (BW_{ir}) as the range of ψ_1 over which $G_{avg}(\psi_1)$ is within 3 dB of its minimum value at 0°. Figure 3 shows the variation of BW_{ir} with N. For $N = 4$, the beamwidth is quite narrow (±48°) but increases to ±59° for $N = 12$. The range is nearly the same as when N increases from 12 to 27, implying the onset of diminishing returns.

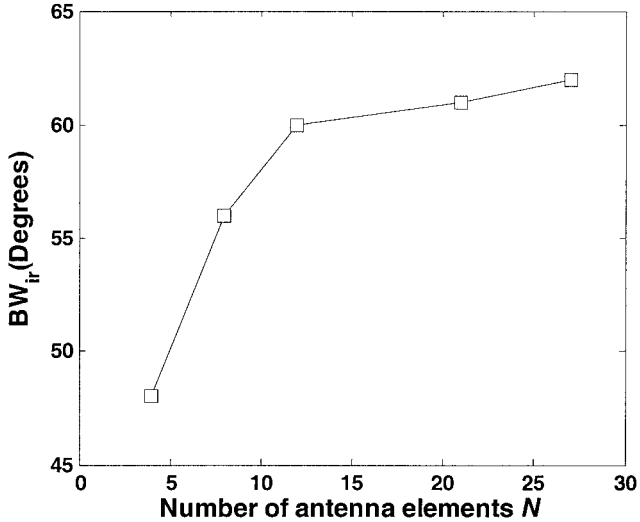

Figure 3 Plot of interference reduction beamwidth (BW_{ir}) with number of antenna elements N ($d = 0.5\lambda$)

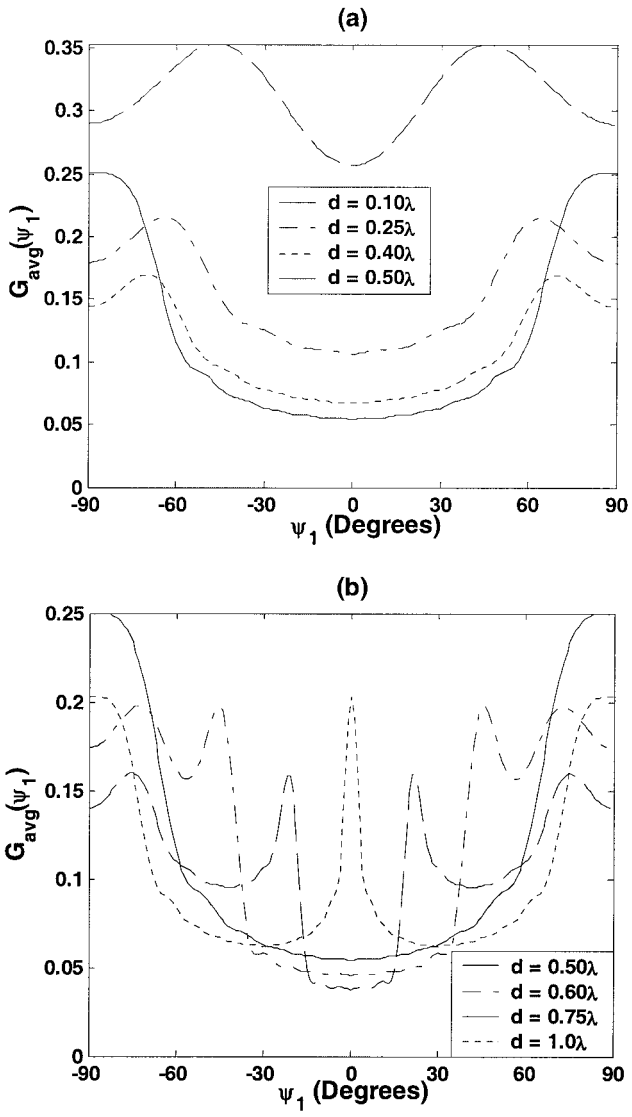

Figure 4 Variation of spatial interference suppression coefficient $G_{avg}(\psi_1)$ with DOA of desired user ψ_1 for an $N = 12$ element linear array for (a) $d = 0.10\lambda$, 0.25λ, 0.40λ, 0.50λ; (b) $d = 0.50\lambda$, 0.60λ, 0.75λ, 1.0λ

Next we investigate the effect of varying the array's inter-element spacing d on $G_{avg}(\psi_1)$. Figure 4 shows the variation of the spatial interference suppression coefficient as a function of inter-element spacing for $N = 12$ element array. From Figure 4(a), we see that interference rejection ability of the array is quite poor when the antenna elements are very tightly spaced ($d \ll 0.5\lambda$). This is because in such a situation, the directivity of the array is reduced and the closely spaced array approximates an omnidirectional antenna. Consequently, the interference rejection property of the array is reduced. As the array elements are moved apart, the interference rejection capability increases, for example, for $d = 0.1\lambda$ the average improvement in SIR at the array output for broadside incidence is $\Delta = 5.9$ dB only, but improves to $\Delta = 11.67$ dB for $d = 0.4\lambda$ and $\Delta = 12.65$ dB for $d = 0.5\lambda$. For $d > 0.5\lambda$, there is formation of grating lobes, which degrade the array performance.

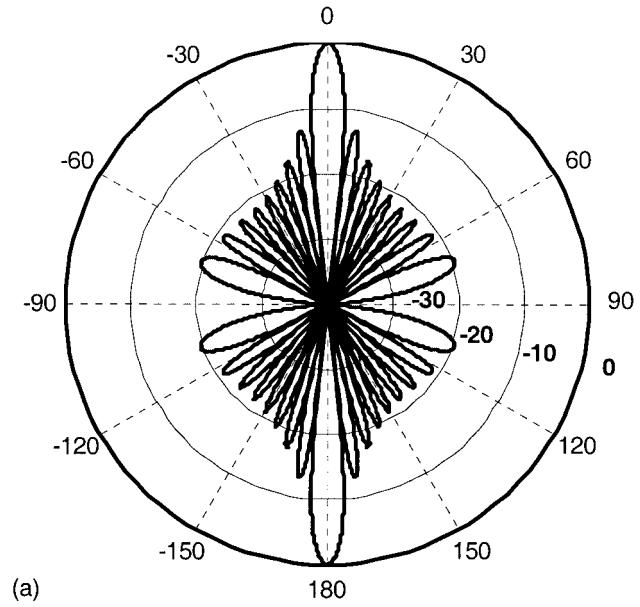

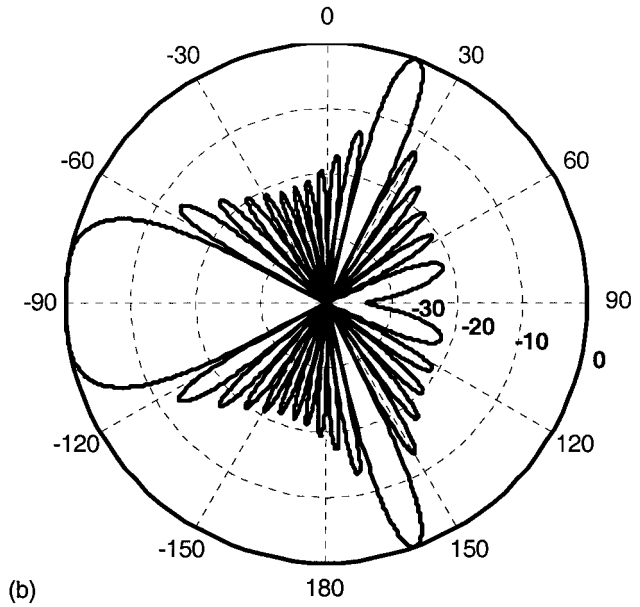

Figure 5 Polar beam pattern plot (dB) for an $N = 12$ element linear array with uniform inter-element spacing $d = 0.75\lambda$ and (a) DOA $\psi_1 = 0°$ (broadside); (b) DOA $\psi_1 = 20°$

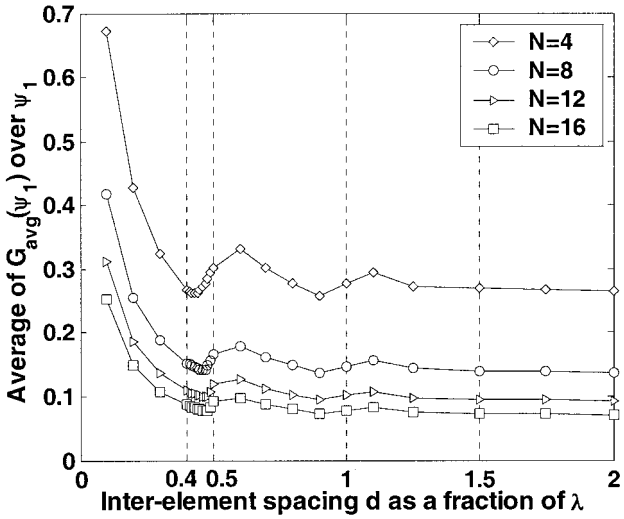

Figure 6 Plot of total average of spatial interference suppression coefficient $G_{avg}(\psi_1)$ over ψ_1 versus inter-element distance d for different number of antenna elements

The apparently complicated shapes of the curves in Figure 4(b) can be explained by looking at the beam patterns for the particular DOAs. Figure 5 shows the beam pattern for an $N = 12$ element array with uniform inter-element spacing $d = 0.75\lambda$ for two steering angles (a) $\psi_1 = 0°$ and (b) $\psi_1 = 20°$. We see that for $\psi_1 = 0°$, the side lobes are narrower, resulting in lower interference being picked up while for $\psi_1 = 20°$, the side lobes are broader as compared to the previous case, resulting in comparatively poorer SIR performance. This can be confirmed by looking at the curve for $d = 0.75\lambda$ in Figure 4(b).

Figure 6 shows the plot of the total average value of $G_{avg}(\psi_1)$ over ψ_1 versus inter-element distance for different number of elements. The results of the curve for an $N = 12$ element array, for example, are obtained by averaging the curves for the different element spacings from Figure 4 over ψ_1. From Figure 6, we see that the optimum value of d (local minimum of the curve) is between 0.4λ and 0.5λ, its exact value depending upon the number of antenna elements. For this separation range ($0.4\lambda < d < 0.5\lambda$), the grating lobes disappear and a fairly narrow beam can be formed on the reference user leading to good performance of the receiving system involving the array.

4. CONCLUSION

This paper presented an analysis concerning the average SIR improvement for linear arrays antennas employed at a base station of a cellular system. It has been shown that the interference rejection capability of the array improves as the number of antenna elements increases. However, increasing the number of elements approximately beyond $N = 12$ results in diminishing returns. It has been shown that for a uniform array the inter-element spacing in the range $0.4\lambda < d < 0.5\lambda$ is optimum in terms of SIR improvement.

REFERENCES

1. S. Choi and D. Yun, Design of adaptive antenna array for tracking the source of maximum power and its application to CDMA mobile communications, IEEE Trans Antennas Propagat AP-45 (1997), 1393–1404.

2. Y.S. Song and H.M. Kwon, Analysis of a simple smart antenna for CDMA wireless communications, Proc IEEE Vehicular Technol Conf, Houston, Texas, 1999, pp. 254–258.
3. S. Durrani and M.E. Bialkowski, Investigation into the performance of an adaptive array in cellular environment, Proc 2002 IEEE AP-S Symp, San Antonio, Texas, 2002.
4. L.C. Godara (Ed.), Handbook of antennas in wireless communications, CRC Press, Boca Raton, Florida, 2002.
5. S. Anderson, M. Millnert, M. Vibergn, and B. Wahlberg, An adaptive array for mobile communication systems, IEEE Trans Antennas Propagat AP-40 (1991), 230–236.

STANDARD AND MICRO GENETIC ALGORITHM OPTIMIZATION OF PROFILED CORRUGATED HORN ANTENNAS

Seelig Sinton, Jacob Robinson, and Yahya Rahmat-Samii
Department of Electrical Engineering
University of California, Los Angeles
Los Angeles, CA 90095-1594

Received 10 June 2002; revised 27 August 2002

ABSTRACT: *The Genetic Algorithm (GA) optimization technique is applied to the optimization of a profiled corrugated horn, designed as a feed for a space-borne remote sensing reflector-antenna system. In addition to using the standard GA (SGA) optimization technique, a profiled corrugated horn is also designed and analyzed using micro GA (μGA). A comparative study has been performed among the various designs.* © 2002 Wiley Periodicals, Inc. Microwave Opt Technol Lett 35: 449–453, 2002; Published online in Wiley InterScience (www.interscience.wiley.com). DOI 10.1002/mop.10635

Key words: *genetic algorithm optimization; micro GA; profiled corrugated horn antennas; offset reflector antennas*

1. INTRODUCTION

While a profiled corrugated horn is an excellent feed for a reflector antenna with high beam efficiency requirements, there are many different parameters, such as the number of corrugations per wavelength and the ratio of the tooth width to groove width, to consider when finding an optimum design. Corrugated horns can be rather heavy and bulky, and it is important to minimize weight without sacrificing the overall performance of the antenna, especially for space-borne applications. One way to optimize a profiled corrugated horn design is to use the genetic algorithm (GA) optimization technique [1]. The GA technique is useful for solving complex multivariable problems; it accepts parameters specified by the user and tries different combinations to find the best design. The best design is the horn that has the highest user-determined fitness function.

Micro GA (μGA) is an optimization technique closely related to GA. μGA works the same way as standard GA (SGA), except that once all the members of a generation have converged within about 5% of each other, the best design is automatically selected for the next generation and the other designs are discarded [2]. The best design participates in the next generation with new randomly selected designs and the evolutionary process continues. In order to take advantage of μGA's restarting feature, a smaller population size than that for SGA is used. A typical SGA population size is usually about 100 members, whereas μGA functions best with a population size of about 10 [2]. Because μGA is repeatedly making random selections, mutation is not used when performing a μGA optimization.

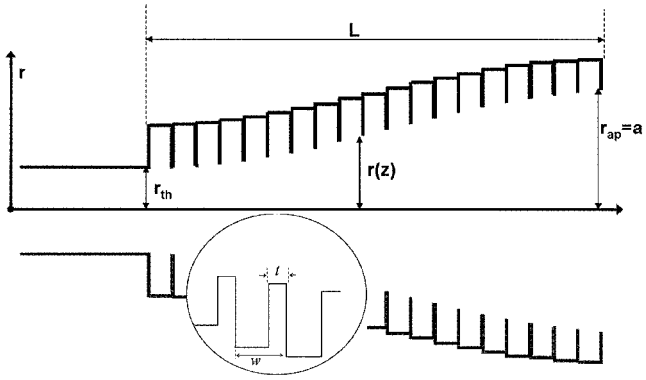

Figure 1 Cross section of a profiled corrugated horn

This paper utilizes the capabilities of SGA and μGA to optimize a profiled corrugated horn to be used as a feed for an offset reflector-antenna system designed for remote sensing of soil moisture from space at the L-band radiometer frequency of 1.414 GHz [3]. The GA program is set up to accept five different parameters and come up with the combination that produces the best design. Additional parameters can also be considered if so desired. The choice of a proper fitness function is highly critical to finding the optimum design. Different fitness functions are evaluated in order to find one that produces a horn that is comparable or better than a horn designed by many trials and errors in a brute-force fashion. Once an acceptable fitness function is established, horns designed using SGA and μGA are compared and contrasted, and the best horn is considered as a feed for an offset reflector-antenna system.

2. OPTIMIZATION PARAMETERS

For the remote sensing application previously mentioned, and taking the physical constraints of the horn design into account, five design parameters are determined by the GA program. The first optimization parameter is the s parameter, which is related to the length of the horn by

$$s = \frac{a^2}{2\lambda L}, \tag{1}$$

where a refers to the horn's aperture radius, λ is the design wavelength, and L is the length of the horn as shown in Figure 1. The second parameter is the number of corrugations per wavelength. The third optimization parameter is the ratio of the tooth width to the total corrugation width (t/w in Fig. 1). The next parameter is the sine profile parameter, A [4]. The value of A is used to define the horn profile:

$$r(z) = r_{th} + (r_{ap} - r_{th})\left[(1 - A)\frac{z}{L} + A \sin^2\left(\frac{\pi z}{2L}\right)\right]. \tag{2}$$

As shown in Figure 1, r_{th} and r_{ap} refer to the radii of the throat and aperture of the horn, respectively. L is the length of the horn and z is the coordinate along the length of the horn in Eq. (2). Typically, A is valued between 0.7 and 0.9 for the best results [5]. The fifth optimization parameter is the matching section parameter γ. This is a value that controls the corrugation depth in the matching section of the corrugated horn. Typically, the matching